Automation in Construction 24 (2012) 213–223

Contents lists available at SciVerse ScienceDirect

Automation in Construction

journal homepage: www.elsevier.com/locate/autcon

A robotic system for underwater eco-sustainable wire-cutting

Rezia M. Molfino *, Matteo Zoppi

University of Genoa, PMAR Robotics, via Opera Pia 15A, 16145 Genoa, Italy

ARTICLE INFO

Article history:
Accepted 9 March 2012
Available online 6 April 2012

Keywords:
Cutting technology
Diamond wire
Marine structures
Underwater robotics

ABSTRACT

The paper deals with the design and development of a diamond wire cutting system used as end-effector of an underwater robot for removal of offshore constructions. This system fulfills the sea-bottom reclamation duties required by the environmental protection acts related to dismissing of off-shore oil plants. The research results have been achieved through extensive interaction between academia and industry, which have solved jointly scientific, technological, economic and social issues along the challenging track to eco-consistency. The, study brings forth: – the analysis of cutting using a diamond wire saw to accomplish the conceptual design of the system; – the wire micro analysis to select a suitable wire configuration. The topics are summarized highlighting the design steps, including preliminary life-cycle assessments accomplished by joining virtual reality tests and trials on an experimental bench. The robotic system has been realized and it is working satisfactory in the North Sea.

1. Introduction

The conventional cutting technologies in use for sub-sea structures, in particular explosives and high-pressure water-jet cutting, disseminate large quantities of pollutants in the sea during the cutting and dismantling process [1–5]. Explosives, especially, brake and disseminate layers of oily mud and drilling residuals stratified in the surroundings of the drilling rig and project fragments are difficult to collect in a wide area.

The change in regulation in the last 10 years practically banned these conventional techniques making urgent the need for effective alternatives. In particular, it was required that, at the end of the dismantling, the seabed was free of any residual structure up to 5 m below the sea-bed surface.

The cutting system presented in the paper was developed in response to these changes in regulations and increasing green attention. It consists of a tool operated by an underwater robot forming a system able to excavate the sea bed soil limiting the volume of the sea-bed materials interested by the excavation; the underwater structures are then cut using diamond wire technology down to 5 m below the sea bottom soil (Fig. 1). Task details can be found in [6–9].

The objectives and key advantages of the selected scientific and technological approach also in comparison to other technologies are:

- the use of a clean technology not interfering with the equilibrium of the marine habitat;
- the absolute certainty to complete the cutting task (unsure with the alternative cutting technologies);
- the optimization in terms of energy, environmental impact, operational efficiency, reliability, diamond wire consumption;
- the automation of the complex tasks involved in the dismantling operations with an “intelligent” remote control/drive station at surface;
- the integrated design of mechanics, hydraulics and the underwater functional components (sensors, electro-hydraulics, data system);
- the unaltered functionality of the portions of structures removed making possible their re-use (impossible with other cutting techniques which cause extensive damages during removal).

The originality of the new system relies in combining and improving known and cooperating technologies, namely: diamond wire cutting and sub-bottom operation with robot-based tools and remote monitoring and control [8,9]. This leads to the unique and never attempted task of shearing below the seabed in a hostile environment with a low-impact duty-scheme (dig-and-saw) through a reliable and safe process (unmanned work-cycles).

The design process took advantage from different kinds of virtual prototyping and simulation techniques [10] that allowed the validation of the analyzed solutions at the subsequent design stages, as decision support and performance verification.

* Corresponding author. Tel.: +39 010 353 2842; fax: +39 010 353 2298.
E-mail addresses: molfino@dimec.unige.it (R.M. Molfino), zoppi@dimec.unige.it (M. Zoppi).

0926-5805/$ – see front matter © 2012 Elsevier B.V. All rights reserved.
doi:10.1016/j.autcon.2012.03.005

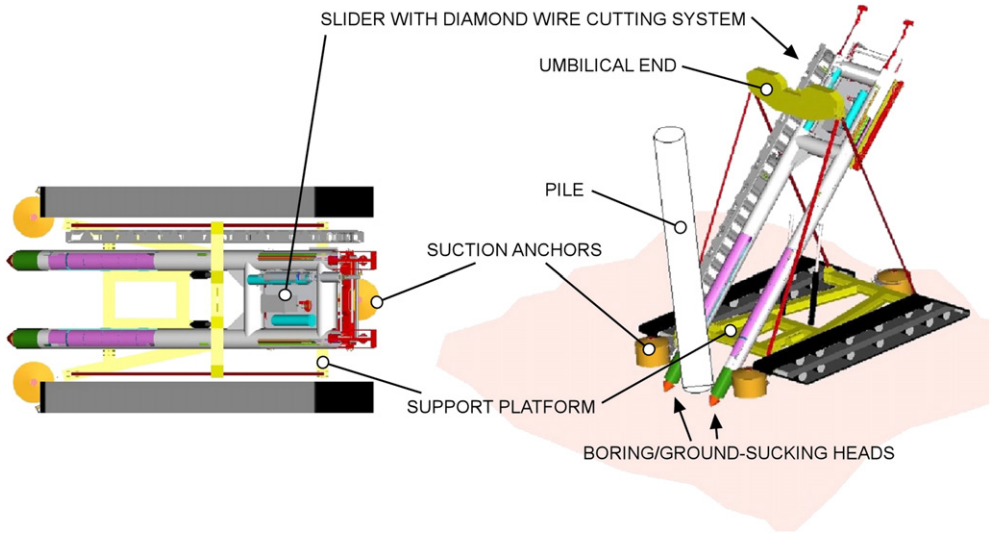

Fig. 1. The robot platform.

The following sections are dedicated to the description of the cutting system macro model and design and to the wire micro model and simulation. The fourth section presents the features of the monitoring and control system. The last section is devoted to field experimental trials with the robotic system prototype.

2. The cutting end-effector

The robot arm comprises two pipes mounted on a slider. A drilling head is present at the free end of each pipe: when activated, they excavate the soil in front of the pipes and the slider can be pushed into the seabed. Two smaller sliders, one per pipe, carry a system of pulleys which tension and run the diamond wire between the pipes. The wire translates along the pipes cutting any body placed in the middle of the pipes.

The success of the remotely operated robotic platform highly depends on the effectiveness and reliability of the diamond wire cutting process. This suggested to deepen the knowledge on the process for typical off-shore structures and on the progression of the wear of wire and beads. A cutting operation cannot be resumed if stopped and the wire must not break during a cut: it is then extremely important to predict the life of the wire.

The study moved in three directions: requirements on arrangement and operative conditions of the wire; adaptation of the wire architecture to materials cut and cutting conditions; beads life prediction by understanding the local properties of the diamond cut action.

To study the wire arrangement and operative conditions, a multibody model of diamond wire loop running on pulleys has been implemented as shown in Fig. 2. The model takes into account the motion of the cutting system along the pipes and the presence and operation of tensioners.

Sealers and a system of water jets clean the wire preventing it from dragging soil inside the pipes when the wire reaches the seabed. To increase cutting reliability and have higher wire pull and cutting rate, a new concept diamond wire string has been studied and adopted.

The adaptation to materials and cutting conditions has shown possible and recommendable to maximize cutting rate and wire life prediction.

Beads life prediction has progressed distinguishing the critical factors into:

- structural properties: bead shaping, diamond laying deposition, diamond size and distribution, metal bond and toughness;
- operation conditions: cutting speed and pressure, cable stretch, diamond crystal fragmentation and edges wear as function of duty parameters.

In the following the models used for defining the new cutting end-effector are briefly introduced.

3. Diamond wire macro analysis

3.1. Wire feeding mechanism

The wire axial tension is a relevant parameter related to wire life and cutting rate. It has been studied using simplified analytic-numerical models implemented in Maple using, as reference, a simplified cutting device equipped with one motorized pulley, as illustrated in Fig. 2. The tension is calculated along the wire and at each pulley.

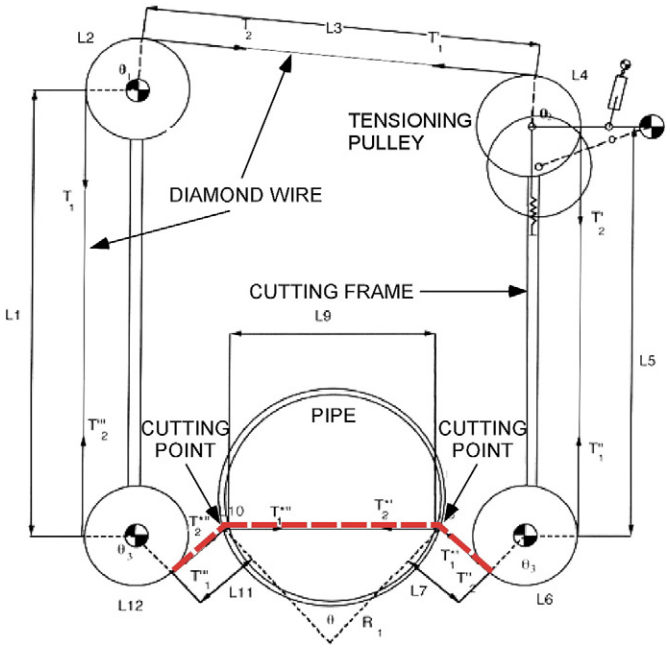

Fig. 2. Configuration of the cutting end-effector.

3.1.1. Motor pulley

The change of axial tension in the wire wrapped around the pulley is exponential and depends on the velocity and linear mass of the wire

3.1.2. Idler pulleys

As for the motor pulley, the axial tension variation along the pulley is exponential but with negative exponent with tension decreasing in the direction of motion. The model shows that the difference in axial tension at the input and output sections of the wire is proportional to the ratio between resistant moment, due to the friction, and pulley radius.

3.1.3. Viscous drag in water

Since the wire moves in water and its velocity is relevant, the viscous drag resistance must be taken into account. It was modeled as proportional to the wire velocity with a coefficient of proportionality estimated experimentally.

3.1.4. Workpiece

The variation of axial tension in the wire in contact with the workpiece has been derived from the model of the idle pulley with an experimental corrective factor acknowledging the sawing action of the beads.

Considering the wire mono-dimensional and linear elastic, the dynamic model of the wire wrapped around the pulley is:

$$F_t dl + dT = \overline{m}\cdot dl\cdot \frac{dv}{dt}$$
$$F_n dl + Td\theta = \overline{m}\cdot dl\cdot \frac{v^2}{R}$$

where T is the tension, $\overline{m}$ the wire mass per unit length, v the wire peripheral speed, $d\theta$ the angle spanned by the wire length dl wrapped around the pulley of radius R, F_t and F_n the tangential and normal force between pulley and wire.

The wire tension varies exponentially along the pulley (the variable θ), then:

$$\frac{T-\overline{m}v^2+sign\left(\frac{dT}{dl}\right)\frac{R}{f}\overline{m}\frac{dv}{dt}}{T_2-\overline{m}v^2+sign\left(\frac{dT}{dl}\right)\frac{R}{f}\overline{m}\frac{dv}{dt}}=e^{-sign\left(\frac{dT}{dl}\right)f(\theta_{H2}-\theta)}=e^{-sign\left(\frac{dT}{dl}\right)f\Delta\theta}$$

where f is the friction factor and $T=T_2$ at $\theta=\theta_{H2}$. In the case of motor pulley, $dT/dl<0$ while, in the case of driven pulley, $dT/dl>0$.

With reference to the terminology introduced in Fig. 2, the set of ten equations below describes the cutting:

$$T=\left(T_2-\overline{m}v^2\right)e^{f\theta_1}+\overline{m}v^2 \text{ motor pulley 1} \quad T_2=T_1-\frac{M_m}{R}$$
$$T=\left(T_2'-\overline{m}v^2\right)e^{-f\theta_2}+\overline{m}v^2 \text{ driven tensioning pulley 2} \quad T_2'=T_1'+\frac{M_r}{R}$$
$$T=\left(T_2''-\overline{m}v^2\right)e^{-f\theta_3}+\overline{m}v^2 \quad T=\left(T_2'''-\overline{m}v^2\right)e^{-f\theta_3}$$
$$+\overline{m}v^2 \text{ driven pulleys 3 and 4} \quad T_2''=T_1''+\frac{M_r}{R};\ T_2'''=T_1'''+\frac{M_r}{R}$$
$$T_1'=T_2+kL_3;\ T_1''=T_2'+kL_5;\ T_1^*=T_2''+kL_7;\ T_1'''=T_2^*+kL_9;$$
$$T_1=T_2'''+kL_1$$
$$T_2^*=T_1^*e^{f'\theta}$$

with f' the friction factor between wire and workpiece considered cylindrical. The * refers to the tension in the wire part performing the cutting operation (in contact with the workpiece). The viscous drag on the wire is modeled by k.

Numerical results for this set of equations have been obtained and a typical result is shown in Fig. 3b.

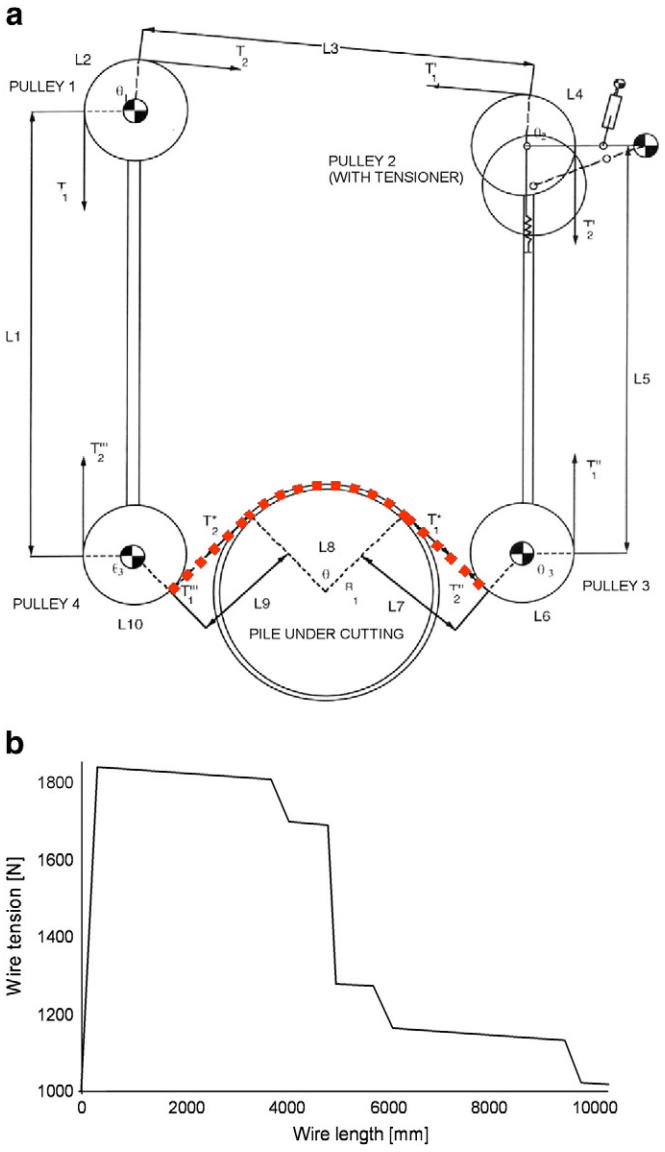

Fig. 3. Reference diamond wire loop (a) and tensions along the wire branches in the initial cutting phase (origin at tension T2) (b).

3.2. Wire tensioning mechanism

A simple and robust tensioning device was designed and its geometry optimized maximizing $\partial T/\partial\alpha$ where α is the tilting angle of the tensioning device.

In order to define the configuration of the cutting system, the case with two motor pulleys was considered and results were compared to the system with one motor pulley. In Fig. 4 the wire tensions are mapped with respect to the tilting angle α. With two motor pulleys, the tension of the wire in the cutting branch is higher and, at same tilting angle, the variation of tension along the cutting branch is higher; also the variation of tension with the tilting angle is higher. The improvement is limited compared to the case with one motor pulley, so finally one motor pulley has been adopted.

3.3. Wire modeling

A multi-body model of the wire has been implemented using the software ADAMS to calculate the contact forces on motor and idle pulleys and the cutting forces (Fig. 5). The friction coefficient at the contact surface workpiece-beads was derived from experimental

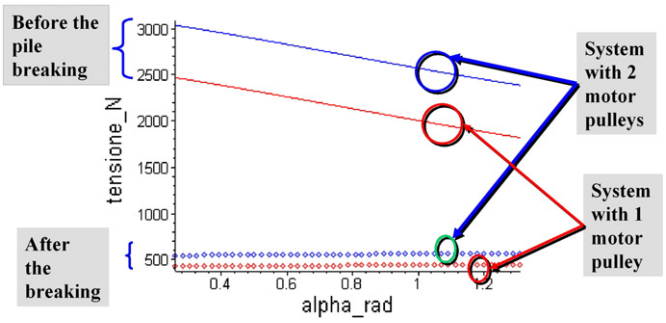

Fig. 4. Wire tensions versus tensioning device tilt angle [rad].

tests with different geometries of the workpiece and different cutting speeds. The wire (Fig. 6a) is modeled as a chain of rigid bodies representing the beads and the wire, connected by rotational joints with flexural stiffness and dumping.

A branch of the wire, constrained at the two ends, is a continuous system with infinite vibration modes and frequencies. The only modes of interest are the ones close to the forcing frequency $\nu_{forcing} = \frac{V_{wire}}{S}$ where S is the spacing of the beads and V the velocity of the wire.

The wire wave model:

$$\mu \frac{\partial^2 \theta}{\partial^2 t} - F \frac{\partial^2 \theta}{\partial^2 x} = 0$$

solved considering the wire constraints is:

$$\theta(x,t) = \left[\theta_{\max} \sin\left(\frac{n\pi}{l_{11}} x\right)\right] \cos\left(\sqrt{F/\mu}\, \frac{n\pi}{l_{11}} t\right)$$

where θ is the vibration amplitude, l_{11} the wire length (see the sketch in Fig. 2), n an integer corresponding to the actual mode, F the applied force and μ the wire mass per unit length. The stationary mechanical waves are described as sinusoidal.

The model has been firstly tuned (values for torsion springs and dumpers) to get the same behavior as the real wire under bending and during free oscillations (measured during physical tests). An intermediate model implemented in the software Pro/Mechanica Motion by PTC has been also used in combination with the ADAMS model (Fig. 6b). After this first calibration, a set of simulations has been run calculating the contact forces between single beads and workpiece during cutting.

Fig. 7 shows the magnitudes of the contact forces between four following beads (numbered 37, 38, 39 and 40) and the workpiece, for one of the cases solved with model fully tuned. The contact between bead 37 and the workpiece starts at time 0.01 s and the reaction force rises till to time 0.03 s when bead 38 contacts the workpiece. At this instant bead 37 oscillates and stabilizes at a force of about 800 N. The bead receives a final strong pulse before detaching from the workpiece. This trend is common to all other beads. The distribution of the contact force vectors obtained is shown in Fig. 6b.

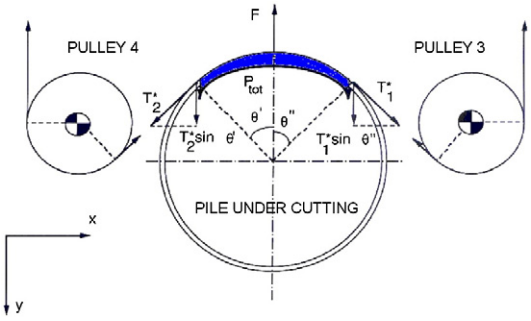

Fig. 5. Contact pressure distribution along the cutting area.

4. Cutting microscopic analysis

4.1. Diamond cutting mechanism and modeling

Each bead can be assimilated to a grindstone with a semi-cylindrical working surface that moves forward along a rectilinear trajectory [11], Fig. 8.

Angles and size of the grain do not have definite values but can be considered probabilistic variables. Generally, the superior draft angle is negative up to −50°, and, consequently, the angle Φ locating the plastic zone is rather small.

The direction of the cutting force spans a wide angle, Ω, with the direction of the wire especially when the contact pressure between wire and workpiece is high. Considering the distance between beads, the ideal shaving (chip) section results very small as well, with shape coefficient rather high. All these elements contribute to increase the cutting pressure increasing the share of mechanical energy converted in heat.

Most of the heat is generated by the rear face of the crystal that crawls on the work-piece because of its small inclination. Since the operation is performed underwater, the temperature of the cutting surfaces keeps low compared to usual cutting temperatures in air-moisture and the removal of shavings from the cutting zone proceeds regularly and efficiently.

The grinding process of the diamond wire can be schematically described as a sequence of short trajectories of each bead during which the bead is in contact with the workpiece. When contacting the workpiece, a subset of the diamond grains on the bead performs the cutting. As time goes by, the cutting edges, and the metal matrix as well, wear out. Gradually the crystals break according to the cleavage surfaces or are completely removed from the matrix.

Critical collisions between the bead flank and the work-piece happen when the cutting wire works on sharp corners as shown in Fig. 8: the wire bends over a certain angle, the spacing spring between consecutive beads crawls on the edge and the collision between bead and corner may damage the bead body.

Such repeated collisions, combined with high thrusting force (wire tension), may induce separation of the bead body from the wire. When this happens, the wire swells up (Fig. 9) and damages quickly; beads fracture and the operative life of the wire shortens suddenly. This working condition must be avoided taking care of the planning of the wire trajectory during the whole cutting process.

The diamond grains used to cut concrete, stones, and other brittle materials have size varying from 175 to 850 μm. The size determines how much a crystal sticks out from the bonding matrix. Edge prominence affects the pitch depth and therefore the overall shaving speed. Bigger crystals can potentially abrade faster and generally are used to work soft materials, whereas the smallest ones have good performance on a tough cut. The grain size is also important as reference to choose the number of edges bonded on the cutting surface and to establish life expectancy and power required: for example, a finer size will increase life expectancy of the tool and power request.

The shape of the crystals varies from octahedron-cubic to irregular structures and grain fragments. A well-defined relation between shape and performance of a diamond exists. A high concentration of irregular and fragmented grains is suggested for light-duty application. On the contrary, a more regular grain with an octahedron-cubic shape is suggested for heavy-duty applications due to the higher breaking resistance. This choice assures a longer life expectancy of the tool and a lower power requirement.

Shock resistance is not only affected by shape and size of the crystals but also by their distribution, density and type of inclusions.

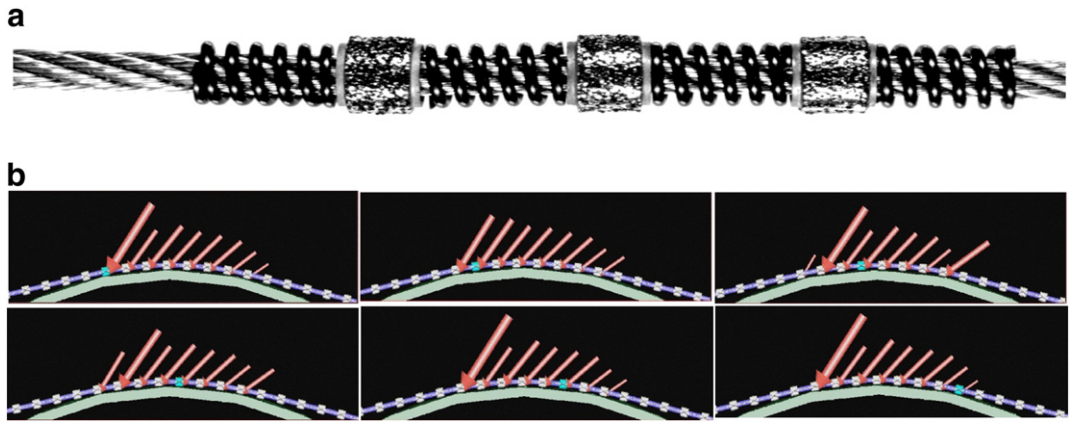

Fig. 6. Wire structure (a) and contact force vectors on the beads during cutting of a curved wall (b).

Generally high shock resistance diamond crystals are necessary to cut hard materials. The presence of a grain rim is another element that contributes to increase breaking probability. Rims reaching the crystal surface form little steps which could be primers of fracture.

The metal bond enveloping the crystals has a very important role to increase wire performance:

- to distribute and to hold firm the diamonds
- to assure a gradual consumption allowing new edges to come out progressively
- to prevent detachment of diamonds
- to dissipate heat
- to distribute shocks and stresses when the beads come in contact with the work-piece.

Low-temperature-bonds, which sinter below 850 °C, do not compromise the mechanical properties of crystals during fabrication. These matrixes are usually composed of cobalt, nickel, iron and bronze. Other types of bond, which need higher sintering temperature over 1000 °C, cause worsening of the diamond properties, mainly shock resistance, and, thus, are not considered for industrial applications.

4.2. Experimental tests

Different kinds of beads and wires have been considered [12,13]. The testing bench realized, Fig. 10, has been used to compare the different designs. In particular, standard and narrow beads wires have been studied to assess the effects of local pressure.

Fig. 11 shows two beads characterized by different geometric parameters: the first (left) has a narrow 6 mm long cylindrical surface covered by the diamond layer; the standard (right) has a wider 10 mm long diamonded surface. The two wires have been tested under same cutting conditions (wire speed, feeding velocity, working pressure, specimen material and size, beads distribution, diamond density).

Comparison results are shown in Fig. 12.

The main result of the tests is that standard beads demonstrate better working performance over time with a smooth loss of cutting capability during the test. On the other hand the beads with new geometry (shorter), with tighter band for diamond crystals deposition, are more effective at the beginning of a cutting cycle but suffer a sudden and faster loss of performance during the operation. This feature limits the application of such wires only to extremely short cuts, for example small components or thin tubes, preventing their use with standard foundation piles that represent the target of the robotic system.

Further results were obtained by microscopic inspection of the diamond crystal deposition in the two cases of standard and new bead design. Focus was on:

- Types of faults of the diamond crystals in the new wire design
- Unsuitable laying of diamonds on the new bond
- Concentration of diamonds
- Percentage of detaching diamonds after use
- Information about any relevant phenomenon related to cutting.

In several cases the distribution of diamonds is homogeneous with the edges of the crystals sticking out from the envelope matrix of the same length (so that the contact forces are well distributed between all edges). In some cases with bigger crystals, edges leaning out more suffer stress concentration and tend to break.

Faults of crystals become more visible at higher magnification. Although not frequently, such faults arise also on new wires. Moreover, these broken diamonds can help the cutting process because cleavage occurs on more than one crystalline plane offering new sharp edges to grind the surface.

The disposition of crystal faces may be not optimal and the sharp edge of many crystals may be sunk in the bond as shown in Fig. 13, left. When the bead touches the work-piece most of these crystals drag on the cutting surface without producing shavings but only heat.

Another example of bad mixing is shown in Fig. 13, right: the upper part is lacking of diamond and, on the contrary, in the lower part there is a too high concentration of crystals with insufficient bonding envelope and consequently detaching quickly from the bead.

Having a general look at the narrow bead behavior, it is possible to notice that the diamond does not worn out or become blunt but it breaks along certain crystalline plains. Anyway this phenomenon is quite marginal and does not justify the drastic decrease of cutting performance (or, better, it could increase the generation of new sharp edges, as mentioned before).

The investigation did separately consider the crystal decay during task progression with respect to cutting pressure and cutting speed.

The cutting pressure, in our case, has an undesired effect on crystal integrity, with fragmentation and powder generation (Fig. 14, left). The cutting speed, whether not properly chosen, compromises the cutting performance.

The most interesting element evidenced by the test execution concerns the presence of a deposition on the bond around the diamonds made of metal oxidation and pieces of broken grains.

The diamond powder formation brings large amounts of original materials into regions no-more active, with rapid decay of the wire life-cycle. The powder formation, however, does not affect the cutting efficiency since the crystals break along sharp cleavage edges (Fig. 14, center). The high speed, when joined to high pressure and to

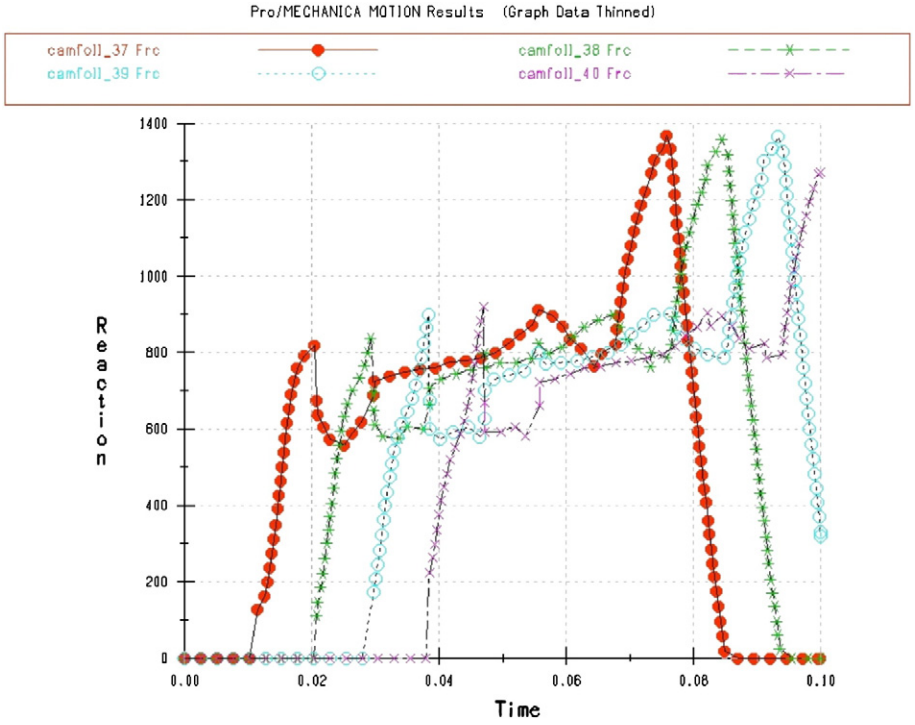

Fig. 7. Simulation results for the contact forces on four following beads (forces in Newton).

diamonds of comparatively large size, progressively drives the crystals inside the supporting bed and modifies the sharp hedges into blunt outlines. The bead surface quickly becomes unsuitable for effective cutting. Side damages, possibly, occur at the bead attack edge, as this undergoes the highest cutting effort, while the subsequent diamonds are removed from too direct actions.

The most interesting aspect concerns the stretching of the matrix and reorientation of crystal faces.

In Fig. 14, right, it is possible to see how the width of the matrix band has significantly increased after the cutting operation. Moreover the figure shows that the central part of the bead cannot contribute to the cutting process since planar surfaces are parallel to the direction of string motion and do not present sharp edges.

Microscopic investigations show clearly that during the cutting process the amount of heat produced by the erosion and the mechanical action on the diamonds cause a relaxation of the nickel matrix that allow the reorientation of the crystals according to the wire direction. This effect significantly decreases string cutting capability since no new sharp edges come in contact with the pile surface. The continuous creeping of the rounded beads on the pile causes metal surface hardening and a new cutting wire has to be used to resume the process.

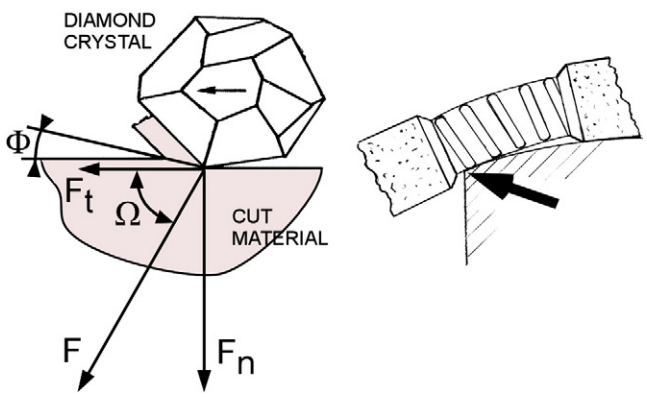

Fig. 8. Single diamond cutting model and wire sketch.

5. Control system and monitoring

The operator, on board the support ship, works at a supervising display with virtual-environment aids useful for decision support, Fig. 15 [14]. The control system provides remote control functionalities for the operator to command step by step the machine and automatic sequences that the operator can launch and the control system executes autonomously. At the end of each sequence the machine reaches a stand-by state. If any trouble or wrong value arises, the control system moves the machine in the stand-by (idle) status, waiting for supervisor decision. In supervision-mode, each single actuator can be commanded allowing the operator to face any unforeseen and accidental situation. The amount of information displayed and the control functions available to the operator are set individually for each control mode. In emergency mode, the value of all sensors is displayed. The emergency mode has access to all functions and can automatically override current tasks by shutting down procedures. The alarms are arranged for a number of parameters; total shut down is enabled only for a limited number of very serious malfunctioning.

The machine is deployed on the seabed by a large ship with crane close to the off-shore structures to dismantle. The same crane used to deploy the machine is used to lift up the pieces cut, one by one, and recover them in the vessel. The cut below seabed is the last step of the dismantling and it is done on the last bottom segments of the foundation piles. Before, the rest of the structure between seabed and surface is cut in pieces using dedicated equipment operating with diamond wire, with simpler architecture since there is no need to dig in the seabed and since this equipment docks directly to the structure to cut, guaranteeing stable and known relative position. After deployment, the machine crawls on the seabed and it is guided from surface to align to the first pile to cut; the frame is secured to the seabed using the vacuum bells at its four corners and the fork is tilted to a suitable angle. The operator sets the feeding speed and wire velocity (on the base of the pile to cut, whose structure is known) and

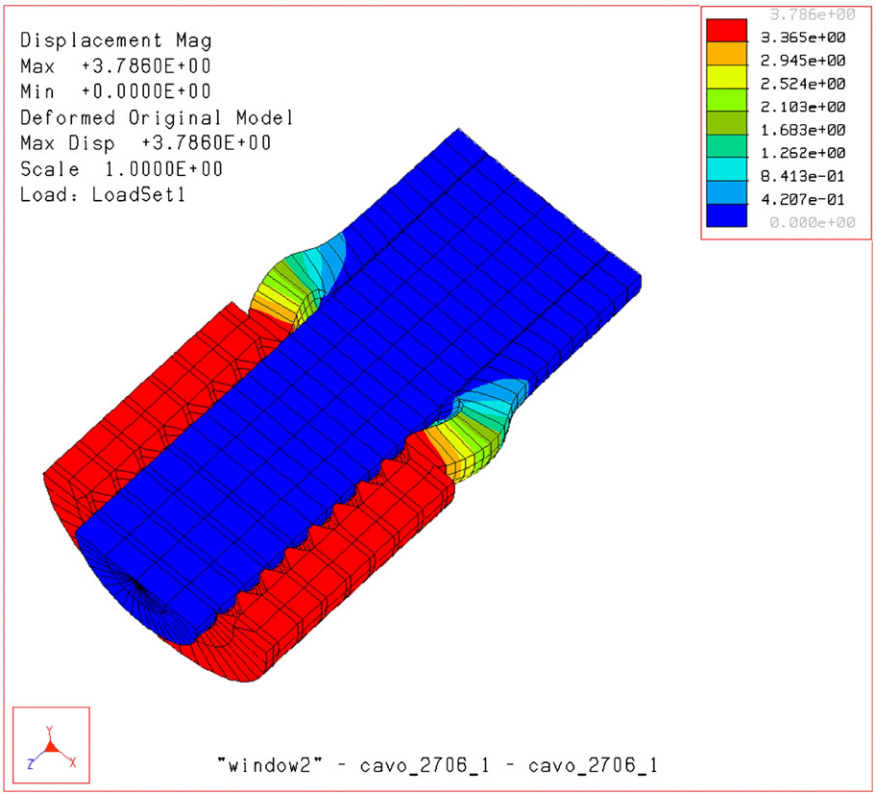

Fig. 9. Swelling of the thermoplastic matrix after bead detachment.

the rest of the sequence is automatic. The pile is hanged to a lifting bag preventing the pile to crush the wire blocking the cut when the cut advances.

The automatic cutting sequence comprises subsequences: Information on the advancement is visualized continuously on the operator interface. At the end of the cutting sequence the machine stops in stand-by status; the pile is lifted to surface by the lifting bag and disappears from the scene; the operator can launch a reset sequence moving back the machine to a ready-for-cut configuration; the machine can be moved to a following pile.

Any new diamond wire is designed to complete the heaviest possible cut (armored foundation pipe with max steel wall thickness and max diameter embraceable by the fork) and it is replaced predictively in the case of use for more cuts; a failure during a cut may still happen and in this case the operator needs to operate on the single movements of the wire slider and pulley system. A wire shear is present to cut blocked wires which cannot be pulled out the workpiece.

The operator has access to several monitored quantities and to a troubleshoot data-base and related hints to select appropriate recovery actions in case of unexpected sequence termination. Only after the operator has checked the emergency and solved the problem, the machine can resume the automatic cycle or shall request further diagnostics or specific actions.

The sensors equipping the machine have been selected in deep underwater class and placed in additional protection cases; they comprise cameras providing a redundant view of the cutting scene and of

Fig. 10. Wire and beads testing facility.

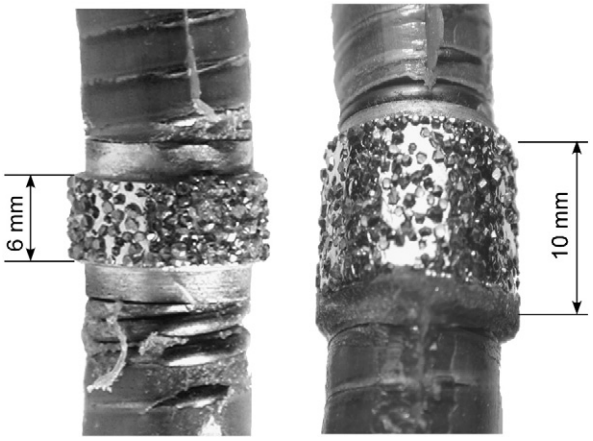

Fig. 11. Narrow (left) and standard (right) diamond beads.

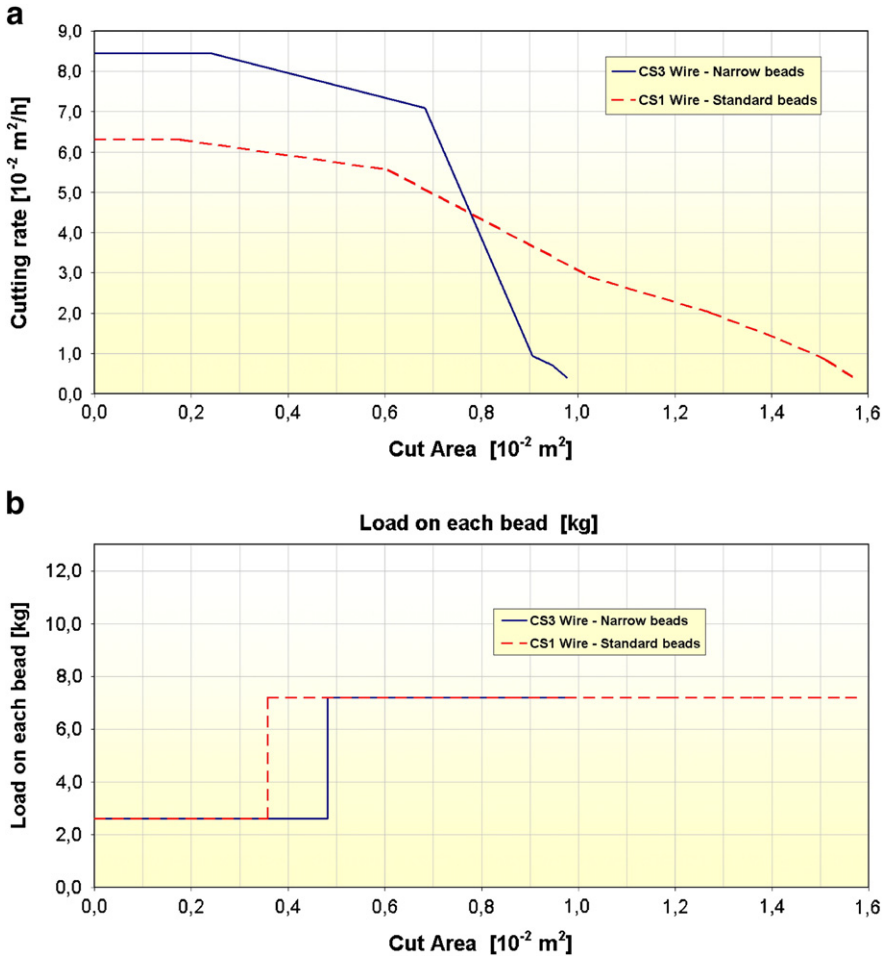

Fig. 12. Comparison between performances of standard (a) and narrow bead wires (b).

the sides and back of the machine, position sensors on all driven axes with redundancy for the critical motions (slider translation and wire speed measured at the two pulleys immediately preceding and following the wire branch performing the cut), water speed at the extremities of the fork and frame to detect and monitor underwater streams affecting stability and motion of the machine, pressure sensors at the docking bells to check the anchorage to the seabed during cutting. The wires of the sensors are routed into steel pipes welded to the frame of the machine for protection against any accidental impact; all pipes reach a common electrical enclosure. The pipes and all enclosures form a closed, sealed circuit filled with oil to prevent sea water to get in; the pressure of the circuit is adapted to the water pressure by a compensation accumulator oil/water with metal diaphragm and open at the water side (positioned on the top back of the frame of the machine close to the main electrical enclosure).

Signal processing algorithms have been developed, coded and checked by simulation to satisfy the stated performance requirements in noisy environment. Each automatic sequence has been sketched, implemented on the 3D model of the vehicle and simulated extensively. Tests on the machine have been done first off water and underwater only when very confident of their reliability in all conditions.

The control system hardware is spread in a surface control unit, including a touch screen computer, a surface-to-underwater interface and an analogical/digital control unit. The sub-sea unit is positioned

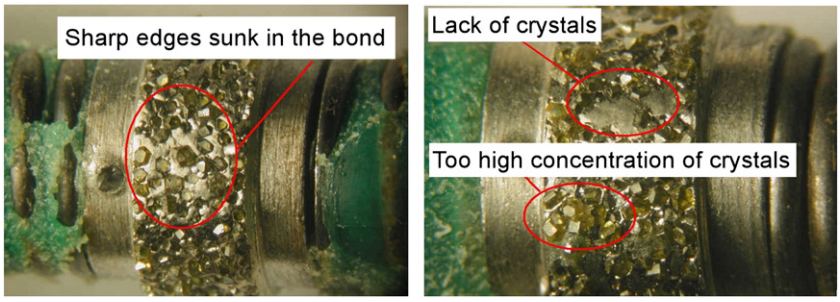

Fig. 13. Anomalies in deposition and distribution of diamond crystals on bead surface.

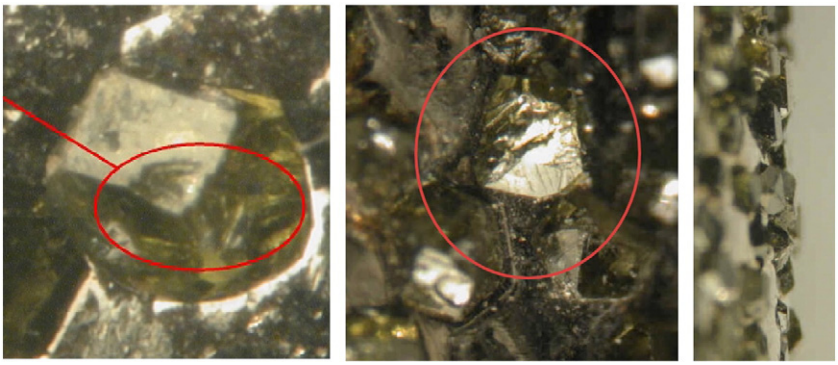

Fig. 14. Diamond crystals cleavage (left) and fragmentation (center); homogeneous reorientation of the diamond surfaces (right).

in the main electrical enclosure and has all onboard electrical equipment connected to it (actuators, sensors, alarm switches, end-stroke/span sensors, cameras). Surface and sub-sea units are connected through an umbilical comprising four power cables for the powering of the machine. In the current implementation twisted wires are used for data transmission (field bus, PROFI or Can) and coaxials for the cameras; reliable fiber optic cables in armored envelope for data transmission are available and will be considered to slim the cable. The umbilical in use is buoyancy neutral; it is secured to the deployment rope used to deploy the machine.

The automatic cutting sequence involves the most critical checks. The parameters monitored are position, feed, tension at the tensioner, wire speed, and forces at the pulleys at the sides of the cutting branch (shear pin loadcells). The control system can be subdivided into three main dynamically coupled subsystems:

- the motion of the frame supporting the diamond wire pulleys (cut feeding)
- the diamond wire tensioning system (pressure of the wire on the pile)
- the diamond wire speed (cutting velocity)
- and a fourth one, the wire cleaning system, which is separately set.

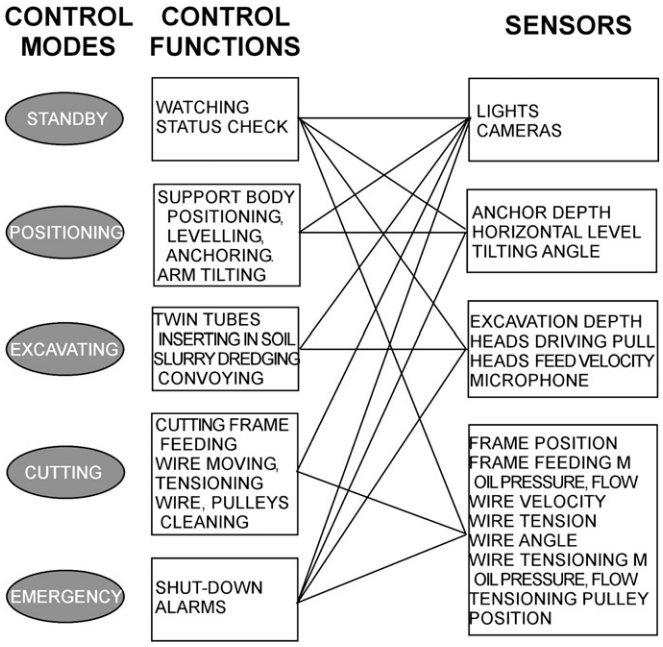

Fig. 15. The cutting system control modes, functions and sensors.

A block diagram of the multi-input multi-output control system (running on board the robotic system) is shown in Fig. 16.

6. Experimental tests on the system prototype

Two groups of experiments have been carried out: on the cutting unit stand alone (the group translating along the fork) and on the whole machine.

The tests on the cutting unit have been carried out on a full scale prototype in a pool on pile trunks representing all typical pile sections present in offshore constructions. The cutting unit tested had the final design, progressively tuned on the base of the test results; it was instrumented and controlled using the same algorithms and schemes in the final machine. The trunks of pile were put in tension to prevent compression of the wire in the advanced phases of the cut due to bending at the cutting section. The aim of the tests was to confirm all decisions on all cutting-related parameters and finalize the design of the unit and its control system; they have been used also to complete the a priori knowledge on the new wires obtained in simulation, as mentioned in the sections discussing the development of the wire.

The tests on the whole machine have been organized in the sea along the North-West reef of the Ulstein, at Ulsteinvik (Fig. 17a,b), Norway. They have comprised final pre-tests with machine out of water to confirm its readiness (in the same way as tests are done on the deck of the support ship before deployment). Then the machine has been deployed in shallow water (50 m) on a sandy seabed similar to typical North Sea soils. The automatic cutting sequence has been launched without pile to test the fork digging with recovery and filtering of the excavated material and the wire running and cleaning in soil. In the same seabed area, steel piles with different section, with and without concrete notch have been positioned replicating typical foundation piles. The tests of the machine have continued on these piles, positioning the machine, tuning the slope of the fork, launching the cutting and recovery sequences. Tests have included cases of wire jamming and blocking with cut of the wire and emergency recovery. Fig. 17c shows one of the piles cut (910 mm diameter, 11 mm thickness, no concrete notch).

Nowadays the robotic system is operative in the North Sea and new open sea services are programmed. The machine is in continuous development by the original consortium who designed and developed it.

7. Conclusions

The European environmental legislation, in particular the Oil Operator and the National Authority act, limits or bans part of the traditional technologies used for the dismantling of off-shore constructions with seabed foundations. It is required to eliminate all foundations up to 5 m below the current seabed level without

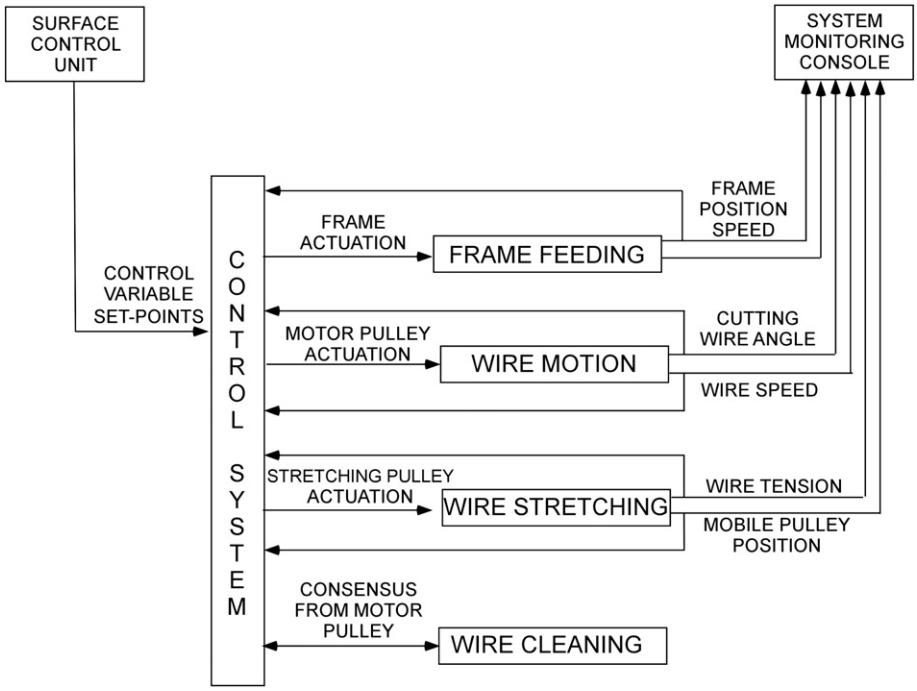

Fig. 16. The reactive cutting system control.

spreading or moving seabed material which may be highly polluting, avoiding explosives and all means impacting on the marine environment. The robotized machine presented, with its original solution of digging fork and diamond wire cutting, is one of the few available technologies today meeting the requirements of the new regulations with strong benefit the oil and gas extraction industry. In addition, the machine developed contributes to remarkable improvement of the working conditions of all personnel involved in the dismantling operations, frequently done in areas with adverse or extreme weather.

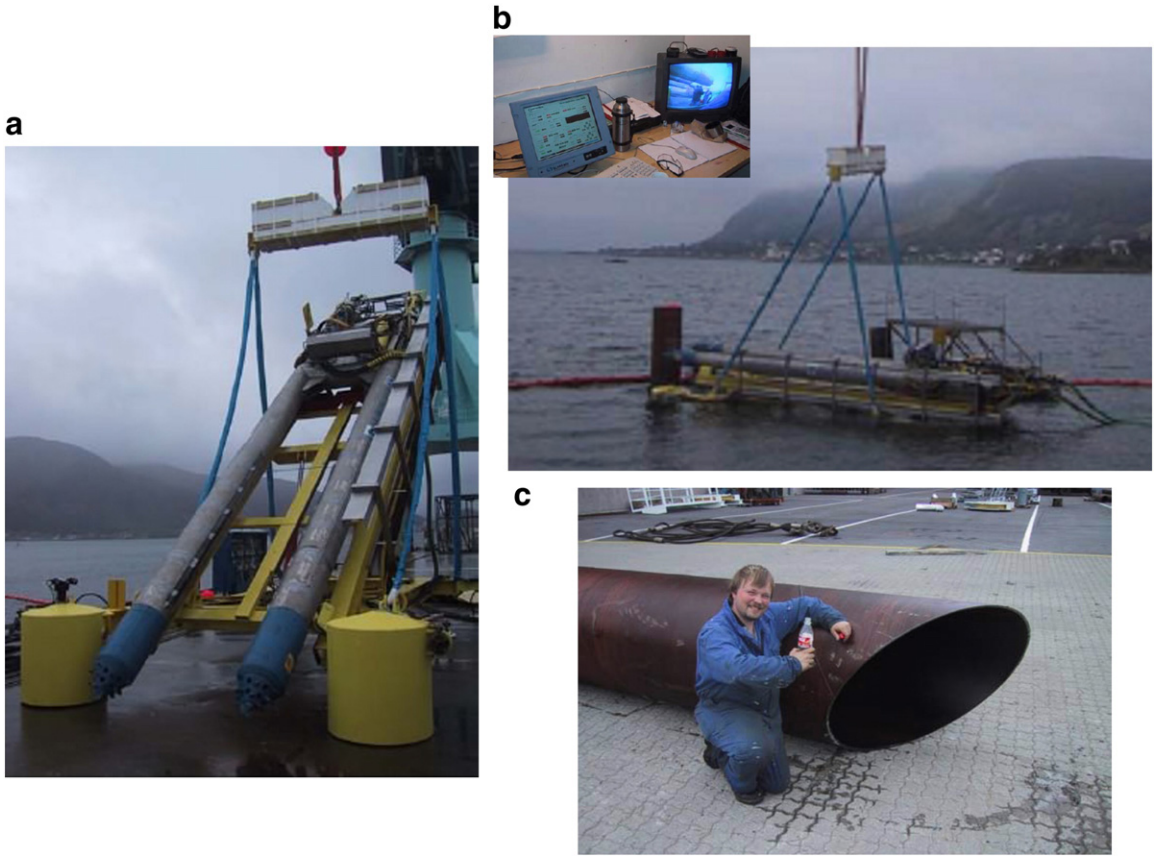

Fig. 17. Robot prototype (a) and its deployment with view of the control room (b); a cut pile (c).

Acknowledgment

This research work was co-funded by the European Commission and ITF consortium. The authors would like to acknowledge Francesco Matteucci and Luigi DeMartino of TS-Tecnospamec for the fruitful suggestions, discussions and cooperation.

References

[1] A. Grant, Toxicity and environmental risk assessment of drill cuttings piles, Decommissioning of Offshore Oil and Gas Installations, IBC Global Conferences, London, 2000.
[2] Phillips Norway Group, Search for best cuttings solution, EPOKE, N° 6, 1999.
[3] PACT Consortium, "PACT consortium awarded Phillips Petroleum Co UK Ltd Maureen platform well abandonments" Press Releases, Dec. 3rd 1999.
[4] Phillips Petroleum Co, "Maureen refloat programme under way" Press Releases, August 5th 1999.
[5] A. Perry, J.E. Snyder, R.C. Byrd, Amoco Eugene Island 367 Jacket Sectioned, Toppled in Place, Offshore, May 1998.
[6] E. Cavallo, R.C. Michelini, R.M. Molfino, A remote-operated robotic platform for underwater decommissioning tasks, 35th Intl. Symposium on Robotics, ISR 2004, Paris, March 23–26 2004, pp. 1–6.
[7] E. Cavallo, R.C. Michelini, R.M. Molfino, A robotic system for off-shore plants decommissioning, IFAC Conference on Control Applications in Marine Systems — CAMS 2004, Ancona, I, 2004, pp. 89–94.
[8] E. Cavallo, R.C. Michelini, R.M. Molfino, R.P. Razzoli, Robotic equipment for deep-sea operation: digital mock-up and assessment, in: G.L. Kovacs, P. Bertok, G. Haidegger (Eds.), Digital Enterprise, New Challenges, Kluver Acad. Pub., Boston, ISBN: 0-7923-7556-4, 2001, pp. 533–542.
[9] M. Callegari, E. Cavallo, E. Garofalo, R.C. Michelini, R.M. Molfino, R.P. Razzoli, The design of diving robots: set-up assessment by virtual mock-ups, Proc. XI ADM Intl. Conf. on Design Tools and Methods in Industrial Engineering, Palermo, vol. C, Dec. 8–12 1999, pp. 147–154.
[10] M.K.A. Hosseini, O. Omidi, A. Meghdari, G. Vossoughi, A composite rigid body algorithm for modeling and simulation of an underwater vehicle equipped with manipulator arms, Journal of Offshore Mechanics and Arctic Engineering 128 (Issue 2) (May 2006) 119–132.
[11] H.K. Tonshoff, H. Hillmann-Apmann, Diamond tools for wire sawing metal components, Report, Institute for Production Engineering and Machine Tools, University of Hannover, Germany, 2001.
[12] R. Molfino, Underwater robotics latest developments and challenges, UV Europe 2007 Shaping the Unmanned Future: Air, Land and Sea Systems, Paris, June 14–15 2007, Shephard CD proceedings.
[13] J. Masood, M. Zoppi, R. Molfino, Application of pseudo-elastic wire for hybrid cutting robotic tool, in: VDE-Verlag (Ed.), 41th International Symposium on Robotics, Munich, Germany, June 7–9 2010.
[14] C.P. Sayers, R.P. Paul, L.L. Whitcomb, D.R. Yoeger, Tele-programming for sub-sea tele-operation, using acoustic communication, IEEE J Oceanic Engineering 23 (1) (January 1998) 60–71.